



11 **Abstract**

12 Assessment of changes in hydrological droughts at specific warming levels (e.g., 1.5
13 or 2 °C) is important for an adaptive water resources management with consideration
14 of the 2015 Paris Agreement. However, most studies focused on the response of
15 drought frequency to the warming and neglected other drought characteristics
16 including severity. By using a semiarid watershed in northern China (i.e., Wudinghe)
17 as an example, here we show less frequent but more severe hydrological drought
18 events emerge at both 1.5 and 2 °C warming levels. We used meteorological forcings
19 from eight Coupled Model Intercomparison Project Phase 5 climate models with four
20 representative concentration pathways, to drive a newly developed land surface
21 hydrological model to simulate streamflow, and analyzed historical and future
22 hydrological drought characteristics based on the Standardized Streamflow Index. The
23 Wudinghe watershed will reach the 1.5 °C (2 °C) warming level around 2006-2025
24 (2019-2038), with an increase of precipitation by 6% (9%) and runoff by 17% (27%)
25 as compared to the baseline period (1986-2005). This results in a drop of drought
26 frequency by 26% (27%). However, the drought severity will rise dramatically by
27 63% (30%), which is mainly caused by the increased variability of precipitation and
28 evapotranspiration. The climate models contribute to more than 82% of total
29 uncertainties in the future projection of hydrological droughts. This study suggests
30 that different aspects of hydrological droughts should be carefully investigated when
31 assessing the impact of 1.5 and 2 °C warming.

32



33 **Key Words:** hydrological drought; global warming; land surface model; CMIP5

34 models; RCP scenarios; uncertainty analysis.

35



36 **1. Introduction**

37 Global warming has affected both natural and artificial systems across continents,
38 bringing a lot of eco-hydrological crises to many countries (Gitay et al., 2002; Tirado
39 et al., 2010; Thornton et al., 2014). The Intergovernmental Panel on Climate Change
40 (IPCC) Fifth Assessment Report (AR5) concluded that global average surface air
41 temperature increased by 0.61 °C in 1986-2005 compared to pre-industrial periods
42 (IPCC, 2014a). In order to mitigate global warming, the Conference of the Parties of
43 the United Nations Framework Convention on Climate Change (UNFCCC)
44 emphasized in the Paris Agreement that the increase in global average temperature
45 should be controlled within 2 °C above preindustrial levels, and further efforts should
46 be made to limit it below 1.5 °C. However, a 2 °C warming would be too high for
47 many regions and countries (James et al., 2017; Rogelj et al., 2015). In addition,
48 whether the temperature controlling goal can be reached is still unknown, with much
49 difficulty under current emission conditions (Peters et al., 2012). Therefore, it is
50 necessary to assess changes in hydrological cycle and extremes under 1.5 and 2 °C
51 temperature increases at regional scale.

52 Global warming is mainly caused by greenhouse gases emissions and has a profound
53 influence on hydrosphere and ecosphere (Barnett et al., 2005; Vorosmarty et al., 2000).
54 It alters hydrological cycle both directly (e.g., influences precipitation and
55 evapotranspiration) and indirectly (e.g., influences plant growth and related
56 hydrological processes) at global (Zhu et al., 2016; McVicar et al., 2012) and local
57 scales (Tang et al., 2013; Zheng et al., 2009; Zhang et al., 2008). Besides affecting the



58 mean states of the hydrological conditions, global warming also intensifies
59 hydrological extremes significantly, such as droughts that were regarded as naturally
60 occurring events when water (precipitation, or streamflow, etc.) is significant below
61 normal over a period of time (Van Loon et al., 2016; Dai, 2011). Among different
62 types of droughts, hydrological droughts focus on the decrease in the availability of
63 water resources, e.g., surface and/or ground water (Lorenzo-Lacruz et al., 2013).
64 Many studies focused on the historical changes, future evolutions, causing factors and
65 uncertainties for hydrological droughts (Chang et al., 2016; Kormos et al., 2016;
66 Orłowsky and Seneviratne, 2013; Parajka et al., 2016; Perez et al., 2011; Prudhomme
67 et al., 2014; Van Loon and Laaha, 2015; Wanders and Wada, 2015; Yuan et al., 2017).
68 Most drought projection studies focused on the future changes over a fixed time
69 period (e.g., the middle and end of the 21st century), but recent studies pointed out the
70 importance on hydrological drought evolution at certain warming levels (Roudier et
71 al., 2016; Marx et al., 2018) given the aim of the Paris Agreement. Moreover, the
72 changes in characteristics (e.g., frequency, duration, severity) of hydrological drought
73 events at specific warming levels received less attention. The projection of these
74 drought characteristics could provide more relevant guidelines for policymakers on
75 implementing adaptation strategies.

76 In the past five decades, a significant decrease in channel discharge was observed in
77 the middle reaches of the Yellow River basin over northern China (Yuan et al., 2018;
78 Zhao et al., 2014), leading to an intensified water resources scarcity in this populated
79 area. In this study, we take a semiarid watershed, the Wudinghe in the middle reaches



80 of the Yellow River basin as a testbed, aiming at solving the following questions: (1)
81 When does temperature increase reach the 1.5 and 2 °C thresholds over the Wudinghe
82 watershed? (2) How do hydrological drought characteristics change at different
83 warming levels? (3) What are the contributions of uncertainties from different sources
84 (e.g., climate models, representative concentration pathways (RCPs) scenarios, and
85 internal variability)?

86 **2. Study area and dataset**

87 In this study, the Wudinghe watershed was selected for hydrological drought analysis.
88 As one of the largest sub-basins of the Yellow River basin, the Wudinghe watershed is
89 located in the Loess Plateau, and has a drainage area of 30261 km² with Baijiachuan
90 hydrological station as the watershed outlet (**Figure 1**). It has a semiarid climate with
91 long-term annual mean precipitation of 356 mm and runoff of 39 mm, resulting in a
92 runoff coefficient of 0.11 (Jiao et al., 2017). Most of the rainfall events are
93 concentrated in summer (June to September) with a large possibility of heavy rains
94 (Mo et al., 2009). Located in the transition zone between cropland/grassland and
95 desert/shrub, the northwest part of Wudinghe watershed is dominated by sandy soil,
96 while the major soil type for the southeast part is loess soil. During recent decades,
97 Wudinghe watershed has experienced a significant streamflow decrease (Yuan et al.,
98 2018; Zhao et al., 2014) and suffered from serious water resource scarcity because of
99 climate change, vegetation degradation and human water consumption (Xiao, 2014;
100 Xu, 2011).
101 The Coupled Model Intercomparison Project Phase 5 (CMIP5) general circulation



102 model (GCM) simulations for historical experiments and future projections formed
103 the science basis for the IPCC AR5 reports (IPCC, 2014b; Taylor et al., 2012). In this
104 study, we chose eight CMIP5 GCMs for historical (1961-2005) and future (2006-2099)
105 drought changing analysis. **Table 1** listed the details of GCMs used in this paper.
106 Because of the deficiency in GCM precipitation and runoff simulations, we used the
107 corrected meteorological forcing data from CMIP5 climate models, to drive a land
108 surface hydrological model to simulate runoff and streamflow (see Section 3.1 for
109 details).

110 All CMIP5 simulations were bias corrected before being used as land surface model
111 input. After interpolating CMIP5 simulations and China Meteorological
112 Administration (CMA) meteorological station observations to a suitable resolution
113 (0.05 degree in this study), a widely used quantile mapping method (Wood et al., 2002;
114 Yuan et al., 2015) was applied to CMIP5/ALL historical simulations to fit its
115 cumulative density functions to observed ones at monthly time scale. For future
116 projections, a modified correction method (Li et al., 2010) was used to remove the
117 biases in CMIP5/RCPs monthly simulations. Bias-corrected monthly precipitation and
118 temperature were then temporally downscaled to a 6-hours interval for driving land
119 surface hydrological model.

120 **3. Land Surface Hydrological Model and Methods**

121 **3.1. Introduction of the CLM-GBHM model**

122 In this study, we chose a newly developed land surface hydrological model,
123 CLM-GBHM, to simulate historical and future streamflow. This model was first



124 developed and applied in Wudinghe watershed at 0.01 degree (Jiao et al., 2017) and
125 then the Yellow River basin at 0.05 degree resolution (Sheng et al., 2017). By
126 improving surface runoff generation, subsurface runoff scheme, river network-based
127 representation and 1-D kinematic wave river routing processes, CLM-GBHM showed
128 good performances in simulating streamflow, soil moisture content and water table
129 depth (Sheng et al., 2017). **Figure 2** demonstrated the structure and main
130 eco-hydrological processes of CLM-GBHM. Model resolution, surface datasets,
131 initial conditions and model parameters were kept the same as Jiao et al. (2017),
132 except that monthly LAI in 1982 was used for all simulations because of an unknown
133 vegetation condition in the future.

134 **3.2. Determination of years reaching specific warming levels**

135 IPCC AR5 (IPCC, 2014a) reported that global average surface air temperature change
136 between pre-industrial period (1850-1900) and reference period (1986-2005) is 0.61
137 (0.55 to 0.67) °C. Therefore, we took 1986-2005 as the baseline period, and used
138 “1.5 °C warming level” referring to a temperature increase of 0.89 (=1.5-0.61) °C
139 compared to the baseline. Similarly, “2 °C warming level” referred to an increase of
140 1.39 (=2-0.61) °C compared to the baseline. As large differences existed in
141 temperature simulations among CMIP5 models and RCP scenarios, we applied a
142 widely used time sampling method (James et al., 2017; Mohammed et al., 2017; Marx
143 et al., 2018) to each GCM under each RCP scenario (referred to as GCM/RCP
144 combination hereafter). A 20-years moving window, which is the length of the
145 baseline period, was used to determine the first period reaching a specific warming



146 level for each combination, with the period median year referred to as the “crossing
147 year”.

148 **3.3. Identification of hydrological drought characteristics**

149 We used a two-step method similar to previous studies (Lorenzo-Lacruz et al., 2013;
150 Ma et al., 2015; Yuan et al., 2017) to extract hydrological drought characteristics in
151 this paper. At the first step, a hydrological drought index named as Standardized
152 Streamflow Index (SSI) was calculated by fitting monthly streamflow using a
153 probabilistic distribution function (Vicente-Serrano et al., 2012; Yuan et al., 2017).
154 Specifically, for each calendar month, historical streamflow values in that month were
155 collected, arranged, and fitted by using a gamma distribution function. Using the same
156 parameters of the fitted gamma distribution, both historical (1961-2005) and future
157 (2006-2099) streamflow values in that calendar month were standardized to get SSI
158 values. The procedure was repeated for twelve calendar months, four RCP scenarios
159 and eight GCMs separately. The second step was identification and characterization of
160 hydrological drought events by a SSI threshold method (Yuan and Wood, 2013;
161 Lorenzo-Lacruz et al., 2013; Van Loon and Laaha, 2015). Here, a threshold of -0.8
162 was selected, which is equivalent to a dry condition with a probability of 20%.
163 Months with SSI below -0.8 were treated as dry months, and 3 or more continuous
164 dry months were considered as the emergence of a hydrological drought event. To
165 characterize the hydrological drought event, drought duration (months) and severity
166 (sum of the difference between -0.8 and SSI) for a certain drought event were
167 calculated.

168 **3.4. Uncertainty separation**

169 Given large spreads among future projections (including combinations of eight GCMs
170 and four RCP scenarios, as shown in shaded areas in **Figure 3**), a separation method
171 (Hawkins and Sutton, 2009; Orłowsky and Seneviratne, 2013) was applied to explore
172 uncertainty from three individual sources, i.e., internal variability, climate models and
173 RCPs scenarios. In order to separate internal variability from other two factors with
174 long-term changing trends included, a 4th order polynomial was selected to fit specific
175 time series twice: (1) obtain an average i_m during historical period (1961-2005) as a
176 reference value, and (2) obtain a smooth fit $x_{m,s,t}$ during the whole period (1961-2099).
177 Future projections ($X_{m,s,t}$) were separated into three parts: reference value (i_m), smooth
178 fit ($x_{m,s,t}$) and residual ($e_{m,s,t}$), and the uncertainties from three sources were then
179 calculated as follows:

$$V = \sum_m \text{var}_{s,t}(e_{m,s,t}) / N_m \quad (1)$$

$$M_t = \sum_s \text{var}_m(x_{m,s,t}) / N_s \quad (2)$$

$$S_t = \text{var}_s(\sum_m x_{m,s,t} / N_m) \quad (3)$$

180 where V , M_t and S_t represent uncertainties from internal variability (which is
181 time-invariant), climate models and RCPs scenarios, N_m and N_s are numbers of
182 climate models and RCPs scenarios, $\text{var}_{s,t}$ denotes the variance across scenarios and
183 time, var_m and var_s are variances across models and scenarios respectively. Finally,
184 uncertainty contributions from each component were calculated as proportions to the
185 sum. In this study, we applied this method to the 20-years moving averaged ensemble
186 time series.



187 **4. Results**

188 **4.1. Changes in hydrometeorology in the past and future**

189 We first calculated the trends during both the historical and future periods for
190 basin-averaged annual mean hydrological variables (Table 2 and **Figure 3**). During
191 1961-2005, there was a significant increasing trend ($p < 0.01$) in observed temperature
192 and a decreasing trend ($p < 0.1$) in observed precipitation, resulted in a decreasing
193 naturalized streamflow ($p < 0.01$) and an increasing hydrological drought frequency
194 ($p < 0.01$). Here, the naturalized streamflow was obtained by adding human water use
195 back to the observed streamflow (Yuan et al., 2017). These historical changes could
196 be captured by hydro-climate model simulations to some extent, although both the
197 warming and drying trends were underestimated (Table 2). During 2006-2099, four
198 variables show consistent changing trends across RCPs scenarios, but with different
199 magnitudes (Table 2). Future temperature and precipitation will increase, resulting in
200 an increasing streamflow and decreasing hydrological drought frequency. Unlike
201 temperature trends that increase from RCP2.6 to RCP8.5 (which indicates different
202 radiative forcings), precipitation trend under RCP6.0 is smaller than that under
203 RCP4.5, suggesting a nonlinear response of regional water cycle to the increase in
204 radiative forcings. As a result, RCP6.0 shows the smallest increasing rate in
205 streamflow and decreasing rate in drought frequency.

206 More details could be found in **Figure 3** when focusing on dynamic changes in the
207 history and future. **Figure 3a** shows that the differences in temperature among RCPs
208 are negligible until 2030s when RCP8.5 starts to outclass other scenarios, and the



209 others begin to diverge in the far future (2060s-2080s). In contrast, differences in
210 future precipitation are small throughout the 21st century, except that RCP8.5 scenario
211 becomes larger after 2080s (**Figure 3b**). As comprehensive outcomes of climate and
212 eco-hydrological factors, a clear decrease-increase pattern in streamflow and an
213 increase-decrease trend in hydrological drought frequency are found (**Figure 3c** and
214 3d). However, differences among RCPs are not discernible. Figures 3b-3d also show
215 that the differences in water-related variables among climate models are very large.

216 **4.2. Determination of time periods crossing 1.5 and 2 °C warming levels**

217 Using the time-sampling method mentioned in Section 3.2, first 20-year periods with
218 mean temperature increasing across 1.5 and 2 °C warming levels for each GCM/RCP
219 combination were identified and listed in **Table 3**. To demonstrate the overall
220 situation for a specific warming level, we chose median year among GCMs as model
221 ensemble for each RCP scenario, and median year among all GCMs and RCPs as total
222 ensemble.

223 As listed in **Table 3**, crossing years for most GCM/RCP combinations reaching 1.5 °C
224 warming level are within 2016-2018 except for GFDL-ESM2M and MRI-CGCM3.
225 Model ensemble years for different RCP scenarios have small differences, and total
226 ensemble year for all GCMs and RCPs is 2016, indicating that 1.5 °C warming level
227 would be reached within 2006-2025 over the Wudinghe watershed generally. As for
228 the 2 °C warming level, there are large differences in crossing year from different
229 GCMs. The crossing years vary from 2016 to 2064 among all combinations, where
230 GFDL-ESM2M and MRI-CGCM3 under RCP2.6 scenario will not reach that



231 warming level (marked as “NR” in **Table 3**, and treated as infinity when calculating
232 median year for the ensemble). Model ensemble years for RCP2.6/4.5/6.0/8.5 are
233 2029/2030/2033/2025 respectively, indicating that the Wudinghe watershed will first
234 reach 2 °C warming level under RCP8.5 and last under RCP6.0 scenario. Overall, the
235 total ensemble year is 2029 for reaching the 2 °C warming level.

236 **4.3. Hydrological changes at 1.5 °C and 2 °C warming levels**

237 After identifying the time periods reaching specific warming levels, we collected
238 precipitation and runoff data within these periods (different among GCM/RCP
239 combinations), and calculated their relative changes compared to the baseline period
240 (1986-2005). **Figure 4** shows the spatial pattern of relative changes in model
241 ensemble mean precipitation. Precipitation increases at both warming levels under all
242 RCP scenarios, while large differences exist in spatial patterns. At 1.5 °C warming
243 level, the watershed-mean changes in precipitation are 5.9% for all scenarios and
244 7.1%/4.7%/6.6%/5.2% for RCP2.6/4.5/6.0/8.5, respectively. Precipitation increases by
245 nearly 10% at 2 °C warming level for all RCP scenarios, except RCP6.0 by 5.9%.
246 Under all scenarios except RCP6.0, Wudinghe watershed has a larger increase in
247 precipitation at 2°C than 1.5 °C warming level. More precipitation increases occur in
248 the south, west and southwest parts which are upstream regions.

249 The watershed-mean runoff increases by 17.0% and 26.6%, which are larger than
250 those of precipitation because of nonlinear hydrological response (Figure 5). At 1.5 °C
251 warming level, RCP6.0 shows greatest runoff increase and RCP4.5 the lowest.
252 Negative changes in runoff emerge in the northeast and southeast regions under



253 RCP4.5 and RCP8.5 (Figure 5), where precipitation increases least (Figure 4).
254 Moving to 2 °C warming level, mean change rates for runoff are over 25% for
255 RCP2.6/4.5/8.5 scenarios, with RCP8.5 the largest (37%). Runoff changes are closed
256 linked to watershed river networks, with large increase in the south and middle parts
257 (upper and middle reaches) and less increase or even decrease in the southeast and
258 northeast parts (lower reaches).

259 **Figure 6** shows the characteristics of hydrological droughts during the baseline period
260 and the periods reaching both warming levels. The number of hydrological drought
261 events averaged among all RCP scenarios and climate models is 10.2 in the baseline
262 period, and it drops to 7.5 (-26% relative to baseline, the same below) at 1.5 °C
263 warming level and 7.4 (-27%) at 2 °C warming level (**Figure 6a**). Hydrological
264 drought durations do not change significantly, with 6.4, 6.7 (+5%) and 6.0 (-6%)
265 months at baseline, 1.5 and 2 °C warming levels, respectively. However, drought
266 severity increases from 2.7 at baseline to 4.4 (+63%) at 1.5 °C warming level, and
267 then to 3.5 (+30%) at 2 °C warming level (**Figure 6a**). These results indicate that
268 although precipitation and runoff increase, the Wudinghe watershed would suffer
269 from more severe hydrological events in the near future at 1.5 °C warming level. The
270 severity could be alleviated in time periods reaching 2 °C warming level, with more
271 precipitation occurring over the watershed.

272 The results for individual scenarios also suggest a decrease in drought frequency, but
273 an increase in drought severity (Figures 6b-6e). The least change in drought severity
274 is found under RCP2.6 scenario (+4%/+15% after warming). Under RCP8.5, drought



275 duration increases from 6.4 to 7.8 (+22%) and 8.6 (+34%) months, and drought
276 severity increases from 2.7 to 5.9 (+119%) and 7.9 (+193%). In short, high emissions
277 would increase the risk of hydrological drought over the Wudinghe watershed
278 significantly through increasing the duration and severity.

279 **5. Discussion**

280 To explore the reason for less frequent but more severe hydrological droughts, we
281 compared the differences in monthly precipitation, evapotranspiration,
282 total/surface/sub-surface runoff and streamflow between baseline and periods
283 reaching 1.5 °C and 2 °C warming levels. Standardized indices for these hydrological
284 variables were used to remove seasonality from monthly time series, and mean values
285 and variabilities of these indices were chosen as indicators.

286 **Figure 7** shows that mean values increase as temperature increases for all
287 standardized hydrological indices, showing a wetter hydroclimate in the near future
288 with more precipitation, evapotranspiration, runoff and streamflow (**Figure 7a**).
289 However, variabilities for the standardized indices in the future are higher than those
290 during baseline period, indicating larger fluctuations and higher chance for extreme
291 droughts/floods at both warming levels (**Figure 7b**). Focusing on the gaps between
292 baseline and future periods (**Figure 7a-7b**), it is clear that the differences in both
293 evapotranspiration and runoff are much larger than those of precipitation for both
294 mean values and standard deviations, suggesting the water redistribution through
295 complicated hydrological processes. The increase in mean value of runoff and
296 consequently streamflow mainly comes from the increase in subsurface runoff. As



297 hydrological drought defined in this paper is based on monthly SSI series, increases in
298 both mean value and variability in precipitation and evapotranspiration indicate a
299 period with less frequent but more severe hydrological drought events.

300 Another issue is the reliability of results considering large differences among CMIP5
301 models. Figure 8 shows the uncertainty fractions contributed from internal variability,
302 climate models and RCPs scenarios based on multi-model and multi-scenario
303 ensemble projections of temperature, precipitation, streamflow and drought frequency.

304 Uncertainty in temperature projection is mainly contributed by climate models before
305 2052, and it is then taken over by RCPs scenarios. Internal variability contributes to
306 less than 3% of the uncertainty for the temperature projection (Figure 8a). For
307 precipitation projection, climate models account for a large proportion of uncertainty
308 (over 73%) throughout the century. The internal variability contributes to larger
309 uncertainty than RCPs scenarios until the second half of the 21st century (Figure 8b).

310 Similar to precipitation, major source of uncertainty for the projections of streamflow
311 and hydrological drought frequency comes from climate models, while the impacts of
312 both internal variability and RCP scenarios are further weakened (Figures 8c-8d).

313 For total ensemble (see **Table 4**), climate model accounts for over 80% of total
314 uncertainties for all variables, while internal variability contributes to a comparable or
315 larger proportion than RCPs scenarios except for temperature. RCPs scenario
316 uncertainty accounts for 18.4% of temperature uncertainty and 4.8% of precipitation
317 uncertainty at 2 °C warming level, both of them are more than doubled compared to
318 those at 1.5 °C warming level. RCPs scenario only contributes to around 3% of the



319 uncertainties in the projections of streamflow and hydrological drought frequency.
320 These results indicate that the improvement in GCMs would largely narrow the
321 uncertainties for future projections of hydrological droughts.
322 There are also some issues for further investigations. As shown in Figure 3, GCM
323 historical simulations underestimates the increasing trend in temperature and
324 decreasing trend in precipitation, and results in underestimations of hydrological
325 drying trends. Although the quantile mapping method used in this study is able to
326 remove the biases in GCM simulations (e.g., mean value, variance), the
327 underestimation of trends could not be corrected. An alternative method is to use
328 regional climate models for dynamical downscaling, which would be useful if
329 regional forcings (e.g., topography, land use change, aerosol emission) are strong.
330 Another issue is about the spatially varied warming rates. IPCC AR5 reported (IPCC,
331 2014c) that global warming for the last 20 years compared to pre-industrial are
332 0.3-1.7 °C (RCP2.6), 1.1-2.6 °C (RCP4.5), 1.4-3.1 °C (RCP6.0), 2.6-4.8 °C (RCP8.5).
333 However, temperature increases vary a lot for different regions. For instance,
334 temperature rises faster in high-altitude (Kraaijenbrink et al., 2017) and polar regions
335 (Bromwich et al., 2013), where the rate of regional warming could be three times of
336 global warming. In this paper, we focused on local warming rates in our studying area
337 with a conclusion that both warming levels could probably be reached in the near
338 future. The reaching periods for regional warming levels are earlier than global mean
339 results (not shown here), which suggest that the hydrological droughts would
340 probably be more severe under global warming of 1.5 and 2 °C scenarios.



341 **6. Conclusions**

342 In this paper, we bias-corrected future projections of meteorological forcings from
343 eight CMIP5 GCM simulations under four RCP scenarios to drive a newly developed
344 land surface hydrological model, CLM-GBHM, to project changes in streamflow and
345 hydrological drought characteristics over the Wudinghe watershed. After determining
346 the local time periods reaching 1.5 °C and 2 °C warming levels for each GCM/RCP
347 combination, we focused on the changes in hydrological drought characteristics at
348 both warming levels. Moreover, projection uncertainties from different sources were
349 separated and analyzed. Main conclusions are listed as follows:

350 (1) With CMIP5 GCM simulations as forcing data, the model ensemble mean hindcast
351 can reproduce the significant decreasing trend of streamflow and increasing trend of
352 hydrological drought frequency in historical period (1961-2005), but the drying trend
353 is underestimated because of GCM uncertainties. Streamflow increases and
354 hydrological drought frequency decreases in the future under all RCP scenarios.

355 (2) The time periods reaching 1.5 °C and 2 °C warming levels over the Wudinghe
356 watershed are 2006-2025 and 2019-2038, respectively. Different RCP scenarios show
357 small deviations in time periods reaching 1.5 °C warming level, while results vary for
358 reaching the 2 °C warming level, with RCP8.5 the earliest and RCP6.0 the latest.

359 (3) Precipitation increases under all RCP scenarios at both warming levels (5.9% and
360 9.0%), while large differences exist in spatial patterns. Runoff has larger relative
361 change rates (17.0% and 26.6%). Large increases of runoff occurred in the upper and
362 middle reaches and less increases or even decreases emerged in the lower reaches,



363 indicating a complex spatial distribution in hydrological droughts.

364 (4) As a result of increasing mean values and variability for precipitation,
365 evapotranspiration and runoff, hydrological drought frequency drops by 26-27% at
366 both warming levels compared to the baseline period, while hydrological drought
367 severity rises dramatically by 63% at 1.5 °C warming level and then drops to 30% at
368 2 °C warming level. This indicates that the Wudinghe watershed would suffer more
369 severe hydrological drought events in the future, especially under RCP6.0 and
370 RCP8.5 scenarios.

371 (5) The main uncertainty sources vary among hydrological variables. In the near
372 future, most uncertainties are from climate models, especially for precipitation. At
373 both warming levels, climate models contribute to over 82% of total uncertainties,
374 while internal variability contributes to a comparable proportion of uncertainties to
375 RCPs scenarios for precipitation, streamflow and hydrological drought frequency.

376

377 **Acknowledgements**

378 This research was supported by National Key R&D Program of China
379 (2018YFA0606002) and National Natural Science Foundation of China (91547103).
380 Daily precipitation and temperature simulated by CMIP5 models were provided by
381 the World Climate Research Programme's Working Group on Coupled Modeling
382 (<https://esgf-data.dkrz.de/search/cmip5-dkrz>). We thank Prof. Dawen Yang and Prof.
383 Huimin Lei for the implementation of the CLM-GBHM land surface hydrological
384 model.

385



386 **References**

- 387 Barnett, T. P., Adam, J. C., and Lettenmaier, D. P.: Potential impacts of a warming
388 climate on water availability in snow-dominated regions, *Nature*, 438, 303-309,
389 doi:10.1038/nature04141, 2005.
- 390 Bromwich, D. H., Nicolas, J. P., Monaghan, A. J., Lazzara, M. A., Keller, L. M.,
391 Weidner, G. A., and Wilson, A. B.: Central West Antarctica among the most
392 rapidly warming regions on Earth, *Nat Geosci*, 6, 139-145,
393 doi:10.1038/Ngeo1671, 2013.
- 394 Chang, J., Li, Y., Wang, Y., and Yuan, M.: Copula-based drought risk assessment
395 combined with an integrated index in the Wei River Basin, China, *Journal of*
396 *Hydrology*, 540, 824-834, doi:10.1016/j.jhydrol.2016.06.064, 2016.
- 397 Dai, A. G.: Drought under global warming: a review, *Wires Clim Change*, 2, 45-65,
398 doi:10.1002/wcc.81, 2011.
- 399 Gitay, H., Suárez, A., Watson, R. T., and Dokken, D. J.: Climate change and
400 biodiversity, IPCC Technical Paper V, 2002.
- 401 Hawkins, E., and Sutton, R.: The Potential to Narrow Uncertainty in Regional
402 Climate Predictions, *B Am Meteorol Soc*, 90, 1095-+,
403 doi:10.1175/2009bams2607.1, 2009.
- 404 IPCC: Climate Change 2013 - The Physical Science Basis, Cambridge University
405 Press, Cambridge, United Kingdom and New York, NY, USA, 1535 pp., 2014a.
- 406 IPCC: Summary for Policymakers, in: Climate Change 2013 - The Physical Science
407 Basis, edited by: Stocker, T. F., Qin, D., Plattner, G.-K., Tignor, M., Allen, S. K.,
408 Boschung, J., Nauels, A., Xia, Y., Bex, V., and Midgley, P. M., Cambridge
409 University Press, Cambridge, United Kingdom and New York, NY, USA, 1-30,
410 2014b.
- 411 IPCC: Long-term Climate Change: Projections, Commitments and Irreversibility, in:
412 Climate Change 2013 - The Physical Science Basis, edited by: Stocker, T. F.,
413 Qin, D., Plattner, G.-K., Tignor, M., Allen, S. K., Boschung, J., Nauels, A., Xia,
414 Y., Bex, V., and Midgley, P. M., Cambridge University Press, Cambridge,



- 415 United Kingdom and New York, NY, USA, 1029-1136, 2014c.
- 416 James, R., Washington, R., Schleussner, C. F., Rogelj, J., and Conway, D.:
417 Characterizing half-a-degree difference: a review of methods for identifying
418 regional climate responses to global warming targets, *Wires Clim Change*, 8,
419 doi:10.1002/wcc.457, 2017.
- 420 Jiao, Y., Lei, H. M., Yang, D. W., Huang, M. Y., Liu, D. F., and Yuan, X.: Impact of
421 vegetation dynamics on hydrological processes in a semi-arid basin by using a
422 land surface-hydrology coupled model, *Journal of Hydrology*, 551, 116-131,
423 doi:10.1016/j.jhydrol.2017.05.060, 2017.
- 424 Kormos, P. R., Luce, C. H., Wenger, S. J., and Berghuijs, W. R.: Trends and
425 sensitivities of low streamflow extremes to discharge timing and magnitude in
426 Pacific Northwest mountain streams, *Water Resour Res*, 52, 4990-5007,
427 doi:10.1002/2015wr018125, 2016.
- 428 Kraaijenbrink, P. D. A., Bierkens, M. F. P., Lutz, A. F., and Immerzeel, W. W.:
429 Impact of a global temperature rise of 1.5 degrees Celsius on Asia's glaciers,
430 *Nature*, 549, 257-+, doi:10.1038/nature23878, 2017.
- 431 Li, H. B., Sheffield, J., and Wood, E. F.: Bias correction of monthly precipitation and
432 temperature fields from Intergovernmental Panel on Climate Change AR4
433 models using equidistant quantile matching, *J Geophys Res-Atmos*, 115,
434 doi:10.1029/2009jd012882, 2010.
- 435 Lorenzo-Lacruz, J., Moran-Tejeda, E., Vicente-Serrano, S. M., and Lopez-Moreno, J.
436 I.: Streamflow droughts in the Iberian Peninsula between 1945 and 2005: spatial
437 and temporal patterns, *Hydrology and Earth System Sciences*, 17, 119-134,
438 doi:10.5194/hess-17-119-2013, 2013.
- 439 Ma, F., Yuan, X., and Ye, A. Z.: Seasonal drought predictability and forecast skill
440 over China, *J Geophys Res-Atmos*, 120, 8264-8275, doi:10.1002/2015jd023185,
441 2015.
- 442 Marx, A., Kumar, R., Thober, S., Rakovec, O., Wanders, N., Zink, M., Wood, E. F.,
443 Pan, M., Sheffield, J., and Samaniego, L.: Climate change alters low flows in
444 Europe under global warming of 1.5, 2, and 3 degrees C, *Hydrology and Earth*



- 445 System Sciences, 22, 1017-1032, doi:10.5194/hess-22-1017-2018, 2018.
- 446 McVicar, T. R., Roderick, M. L., Donohue, R. J., Li, L. T., Van Niel, T. G., Thomas,
447 A., Grieser, J., Jhajharia, D., Himri, Y., Mahowald, N. M., Mescherskaya, A. V.,
448 Kruger, A. C., Rehman, S., and Dinpashoh, Y.: Global review and synthesis of
449 trends in observed terrestrial near-surface wind speeds: Implications for
450 evaporation, Journal of Hydrology, 416, 182-205,
451 doi:10.1016/j.jhydrol.2011.10.024, 2012.
- 452 Mo, X. G., Liu, S. X., Chen, D., Lin, Z. H., Guo, R. P., and Wang, K.: Grid-size
453 effects on estimation of evapotranspiration and gross primary production over a
454 large Loess Plateau basin, China, Hydrolog Sci J, 54, 160-173,
455 doi:10.1623/hysj.54.1.160, 2009.
- 456 Mohammed, K., Islam, A. S., Islam, G. M. T., Alfieri, L., Bala, S. K., and Khan, M. J.
457 U.: Extreme flows and water availability of the Brahmaputra River under 1.5 and
458 2 A degrees C global warming scenarios, Climatic Change, 145, 159-175,
459 doi:10.1007/s10584-017-2073-2, 2017.
- 460 Orłowsky, B., and Seneviratne, S. I.: Elusive drought: uncertainty in observed trends
461 and short- and long-term CMIP5 projections, Hydrology and Earth System
462 Sciences, 17, 1765-1781, doi:10.5194/hess-17-1765-2013, 2013.
- 463 Parajka, J., Blaschke, A. P., Bloeschl, G., Haslinger, K., Hepp, G., Laaha, G.,
464 Schoener, W., Trautvetter, H., Viglione, A., and Zessner, M.: Uncertainty
465 contributions to low-flow projections in Austria, Hydrology and Earth System
466 Sciences, 20, 2085-2101, doi:10.5194/hess-20-2085-2016, 2016.
- 467 Perez, G. A. C., van Huijgevoort, M. H. J., Voss, F., and van Lanen, H. A. J.: On the
468 spatio-temporal analysis of hydrological droughts from global hydrological
469 models, Hydrology and Earth System Sciences, 15, 2963-2978,
470 doi:10.5194/hess-15-2963-2011, 2011.
- 471 Peters, G. P., Andrew, R. M., Boden, T., Canadell, J. G., Ciais, P., Le Quéré, C.,
472 Marland, G., Raupach, M. R., and Wilson, C.: The challenge to keep global
473 warming below 2 C, Nat Clim Change, 3, 4, 2012.
- 474 Prudhomme, C., Giuntoli, I., Robinson, E. L., Clark, D. B., Arnell, N. W., Dankers,



- 475 R., Fekete, B. M., Franssen, W., Gerten, D., Gosling, S. N., Hagemann, S.,
476 Hannah, D. M., Kim, H., Masaki, Y., Satoh, Y., Stacke, T., Wada, Y., and
477 Wisser, D.: Hydrological droughts in the 21st century, hotspots and uncertainties
478 from a global multimodel ensemble experiment, *Proceedings of the National*
479 *Academy of Sciences*, 111, 3262-3267, doi:10.1073/pnas.1222473110, 2014.
- 480 Rogelj, J., Luderer, G., Pietzcker, R. C., Kriegler, E., Schaeffer, M., Krey, V., and
481 Riahi, K.: Energy system transformations for limiting end-of-century warming to
482 below 1.5 degrees C, *Nat Clim Change*, 5, 519+, doi:10.1038/nclimate2572,
483 2015.
- 484 Roudier, P., Andersson, J. C. M., Donnelly, C., Feyen, L., Greuell, W., and Ludwig,
485 F.: Projections of future floods and hydrological droughts in Europe under a+2
486 degrees C global warming, *Climatic Change*, 135, 341-355,
487 doi:10.1007/s10584-015-1570-4, 2016.
- 488 Sheng, M. Y., Lei, H. M., Jiao, Y., and Yang, D. W.: Evaluation of the Runoff and
489 River Routing Schemes in the Community Land Model of the Yellow River
490 Basin, *J Adv Model Earth Sy*, 9, 2993-3018, doi:10.1002/2017ms001026, 2017.
- 491 Tang, Y., Tang, Q., Tian, F., Zhang, Z., and Liu, G.: Responses of natural runoff to
492 recent climatic variations in the Yellow River basin, China, *Hydrology and Earth*
493 *System Sciences*, 17, 4471-4480, doi: 10.5194/hess-17-4471-2013, 2013.
- 494 Taylor, K. E., Stouffer, R. J., and Meehl, G. A.: An Overview of Cmp5 and the
495 Experiment Design, *B Am Meteorol Soc*, 93, 485-498,
496 doi:10.1175/Bams-D-11-00094.1, 2012.
- 497 Thornton, P. K., Ericksen, P. J., Herrero, M., and Challinor, A. J.: Climate variability
498 and vulnerability to climate change: a review, *Global Change Biol*, 20,
499 3313-3328, doi:10.1111/gcb.12581, 2014.
- 500 Tirado, M. C., Clarke, R., Jaykus, L. A., McQuatters-Gollop, A., and Franke, J. M.:
501 Climate change and food safety: A review, *Food Res Int*, 43, 1745-1765,
502 doi:10.1016/j.foodres.2010.07.003, 2010.
- 503 Van Loon, A. F., and Laaha, G.: Hydrological drought severity explained by climate
504 and catchment characteristics, *Journal of Hydrology*, 526, 3-14,



- 505 doi:10.1016/j.jhydrol.2014.10.059, 2015.
- 506 Van Loon, A. F., Stahl, K., Di Baldassarre, G., Clark, J., Rangelcroft, S., Wanders, N.,
507 Gleeson, T., Van Dijk, A. I. J. M., Tallaksen, L. M., Hannaford, J., Uijlenhoet, R.,
508 Teuling, A. J., Hannah, D. M., Sheffield, J., Svoboda, M., Verbeiren, B.,
509 Wagener, T., and Van Lanen, H. A. J.: Drought in a human-modified world:
510 reframing drought definitions, understanding, and analysis approaches,
511 Hydrology and Earth System Sciences, 20, 3631-3650,
512 doi:10.5194/hess-20-3631-2016, 2016.
- 513 Vicente-Serrano, S. M., Lopez-Moreno, J. I., Begueria, S., Lorenzo-Lacruz, J.,
514 Azorin-Molina, C., and Moran-Tejeda, E.: Accurate Computation of a
515 Streamflow Drought Index, J Hydrol Eng, 17, 318-332,
516 doi:10.1061/(Asce)He.1943-5584.0000433, 2012.
- 517 Vorosmarty, C. J., Green, P., Salisbury, J., and Lammers, R. B.: Global water
518 resources: Vulnerability from climate change and population growth, Science,
519 289, 284-288, doi:10.1126/science.289.5477.284, 2000.
- 520 Wanders, N., and Wada, Y.: Human and climate impacts on the 21st century
521 hydrological drought, Journal of Hydrology, 526, 208-220,
522 doi:10.1016/j.jhydrol.2014.10.047, 2015.
- 523 Wood, A. W., Maurer, E. P., Kumar, A., and Lettenmaier, D. P.: Long-range
524 experimental hydrologic forecasting for the eastern United States, J Geophys
525 Res-Atmos, 107, doi:10.1029/2001jd000659, 2002.
- 526 Xiao, J. F.: Satellite evidence for significant biophysical consequences of the "Grain
527 for Green" Program on the Loess Plateau in China, J Geophys Res-Bioge, 119,
528 2261-2275, doi:10.1002/2014jg002820, 2014.
- 529 Xu, J. X.: Variation in annual runoff of the Wudinghe River as influenced by climate
530 change and human activity, Quatern Int, 244, 230-237,
531 doi:10.1016/j.quaint.2010.09.014, 2011.
- 532 Yuan, X., and Wood, E. F.: Multimodel seasonal forecasting of global drought onset,
533 Geophys Res Lett, 40, 4900-4905, doi:10.1002/grl.50949, 2013.
- 534 Yuan, X., Roundy, J. K., Wood, E. F., and Sheffield, J.: Seasonal forecasting of



- 535 global hydrologic extremes: system development and evaluation over GEWEX
536 basins, *B Am Meteorol Soc*, 96, 1895-1912, doi:10.1175/BAMS-D-14-00003.1,
537 2015.
- 538 Yuan, X., Zhang, M., Wang, L. Y., and Zhou, T.: Understanding and seasonal
539 forecasting of hydrological drought in the Anthropocene, *Hydrology and Earth
540 System Sciences*, 21, 5477-5492, doi:10.5194/hess-21-5477-2017, 2017.
- 541 Yuan, X., Y. Jiao, D. Yang, and H. Lei: Reconciling the attribution of changes in
542 streamflow extremes from a hydroclimate perspective, *Water Resour Res*,
543 doi:10.1029/2018WR022714, 2018
- 544 Zhang, X. P., Zhang, L., Zhao, J., Rustomji, P., and Hairsine, P.: Responses of
545 streamflow to changes in climate and land use/cover in the Loess Plateau, China,
546 *Water Resour Res*, 44, doi:10.1029/2007wr006711, 2008.
- 547 Zhao, G. J., Tian, P., Mu, X. M., Jiao, J. Y., Wang, F., and Gao, P.: Quantifying the
548 impact of climate variability and human activities on streamflow in the middle
549 reaches of the Yellow River basin, China, *Journal of Hydrology*, 519, 387-398,
550 doi:10.1016/j.jhydrol.2014.07.014, 2014.
- 551 Zheng, H. X., Zhang, L., Zhu, R. R., Liu, C. M., Sato, Y., and Fukushima, Y.:
552 Responses of streamflow to climate and land surface change in the headwaters of
553 the Yellow River Basin, *Water Resour Res*, 45, doi:10.1029/2007wr006665,
554 2009.
- 555 Zhu, Z. C., Piao, S. L., Myneni, R. B., Huang, M. T., Zeng, Z. Z., Canadell, J. G.,
556 Ciais, P., Sitch, S., Friedlingstein, P., Arneeth, A., Cao, C. X., Cheng, L., Kato, E.,
557 Koven, C., Li, Y., Lian, X., Liu, Y. W., Liu, R. G., Mao, J. F., Pan, Y. Z., Peng,
558 S. S., Penuelas, J., Poulter, B., Pugh, T. A. M., Stocker, B. D., Viovy, N., Wang,
559 X. H., Wang, Y. P., Xiao, Z. Q., Yang, H., Zaehle, S., and Zeng, N.: Greening of
560 the Earth and its drivers, *Nat Clim Change*, 6, 791-795,
561 doi:10.1038/nclimate3004, 2016.



562 **Figure Captions**

563 **Figure 1.** Location, elevation and river networks for the Wudinghe watershed.

564 **Figure 2.** Structure and main eco-hydrological processes for the land surface
565 hydrological model CLM-GBHM. (modified from Jiao et al., 2017)

566 **Figure 3.** Historical (ALL) and future (RCP2.6/4.5/6.0/8.5) time series of
567 standardized annual mean (a) temperature, (b) precipitation and (c) streamflow, and (d)
568 the time series of hydrological drought frequency (drought months for each year) over
569 the Wudinghe watershed. Shaded areas indicate the ranges between maximum and
570 minimum values among CMIP5/CLM-GBHM model simulations. ALL represents
571 historical simulations with both anthropogenic and natural forcings,
572 RCP2.6/4.5/6.0/8.5 represent four representative concentration pathways from lower
573 to higher emission scenarios.

574 **Figure 4.** Spatial pattern of relative changes in multi-model ensemble mean
575 precipitation at 1.5 °C and 2 °C warming levels compared to the baseline period
576 (1986-2005). The percentages in the upper-right corners of each panel are the
577 watershed-mean changes for different RCP scenarios, and the percentages in the top
578 brackets are the mean values from four RCP scenarios.

579 **Figure 5.** The same as **Figure 4**, but for the spatial patterns of runoff changes.

580 **Figure 6.** Comparison of the characteristics (frequency (number of drought events per
581 20 years), duration (months) and severity) averaged among climate models and RCP
582 scenarios for hydrological drought events during the baseline period (1986-2005) and
583 the periods reaching 1.5 °C and 2 °C warming levels.



584 **Figure 7.** Comparison of (a) mean values and (b) standard deviations for hydrological
585 indices averaged among climate models and RCP scenarios during the baseline period
586 (1986-2005) and the periods reaching 1.5 °C and 2 °C warming levels. SPI, SEI, SRI,
587 SSRI, SBI, SSI represent standardized indices of precipitation, evapotranspiration,
588 runoff, surface runoff, baseflow (subsurface runoff) and streamflow, respectively.

589 **Figure 8.** Fractions of uncertainties from internal variability (orange), RCP scenarios
590 (green) and climate models (blue) for the projections of 20-years moving averaged (a)
591 temperature, (b) precipitation (c) streamflow and (d) hydrological drought frequency.
592 Two dashed lines indicate the multi-model ensemble median years reaching 1.5 °C
593 (year 2016) and 2 °C (year 2029) warming levels, respectively.

594

595 **Table Captions**

596 **Table 1.** CMIP5 model simulations used in this study. ALL represents historical
597 simulations with both anthropogenic and natural forcings (r1i1p1 realization),
598 RCP2.6/4.5/6.0/8.5 represent four representative concentration pathways from lower
599 to higher emission scenarios.

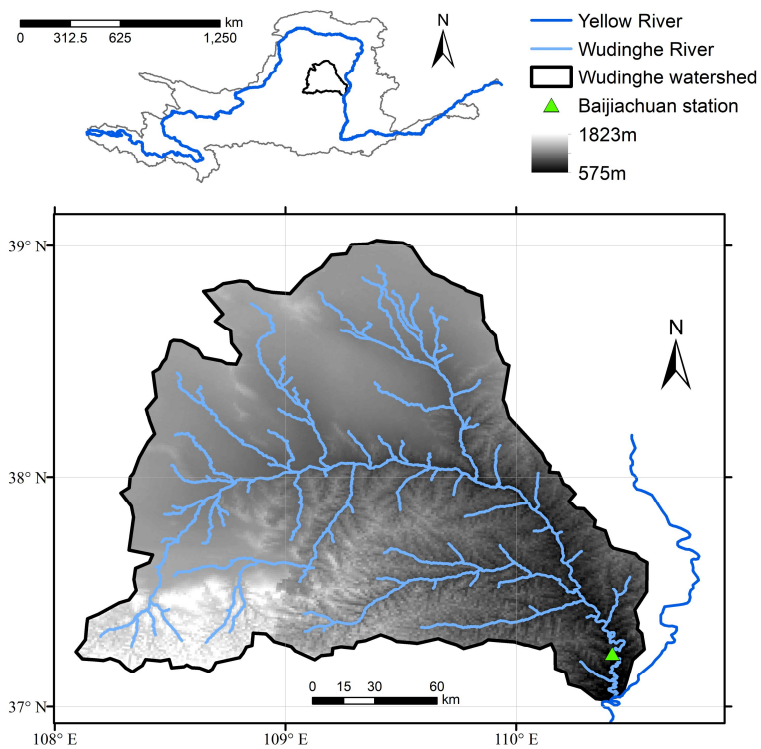
600 **Table 2.** Trends in hydrometeorological variables and hydrological drought frequency
601 over the Wudinghe watershed. Historical observed trends for streamflow and drought
602 frequency were calculated by using naturalized streamflow data (Yuan et al., 2017).
603 Here, “*” and “**” indicate 90% and 99% confidence levels, respectively, while those
604 without any “*” show no significant changes ($p > 0.1$).

605 **Table 3.** Determination of crossing year for the periods reaching 1.5°C and 2 °C



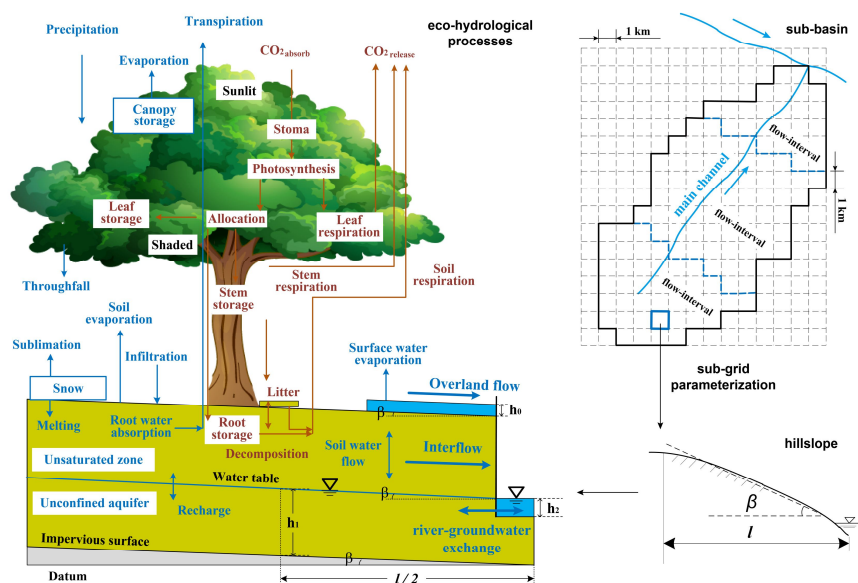
606 warming levels for different GCMs and RCPs combinations. Here, “NR” means that
607 the corresponding GCM/RCP combination will not reach the specified warming level
608 throughout the 21st century.

609 **Table 4.** Uncertainty contributions (%) from internal variability, climate models and
610 RCPs scenarios for the future projections considering 1.5 °C and 2 °C warming levels.



611

612 **Figure 1.** Location, elevation and river networks for the Wudinghe watershed.

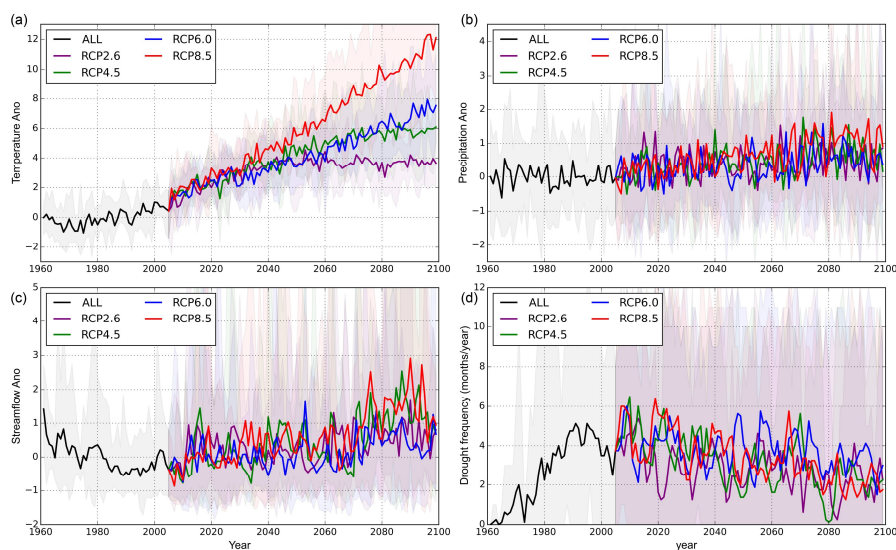


613

614 **Figure 2.** Structure and main eco-hydrological processes for the land surface

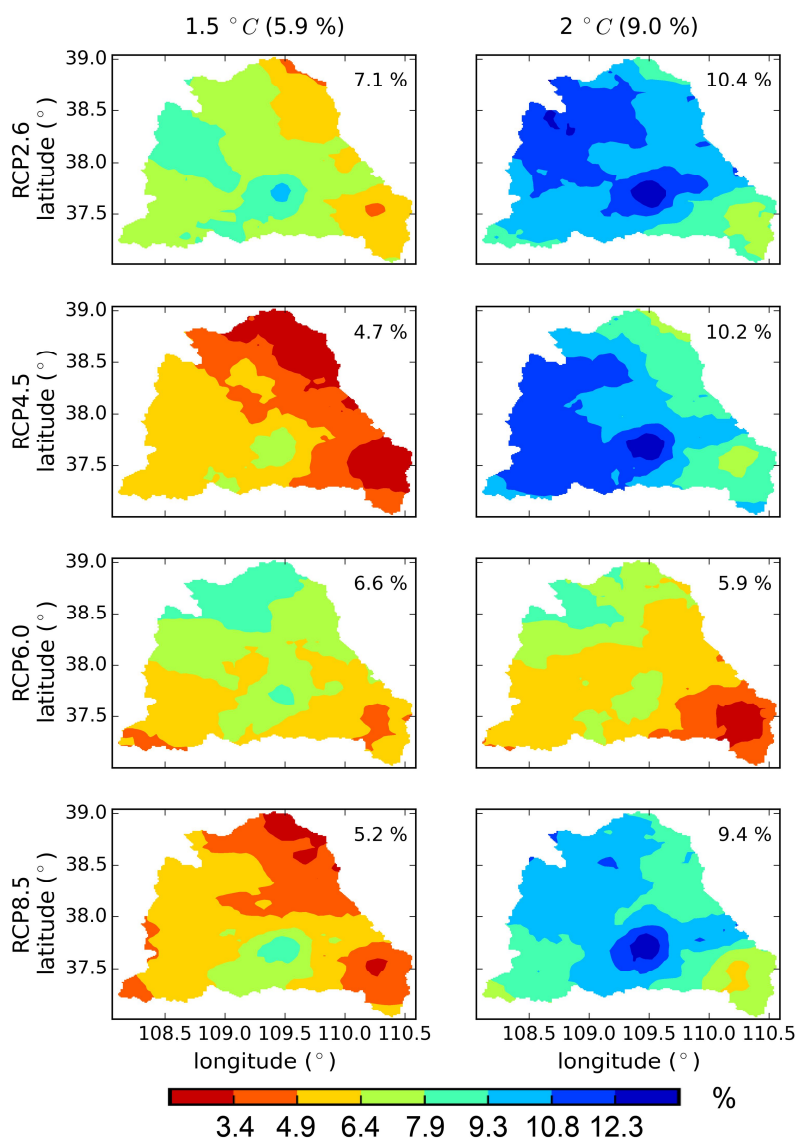
615 hydrological model CLM-GBHM. (modified from Jiao et al., 2017)

616



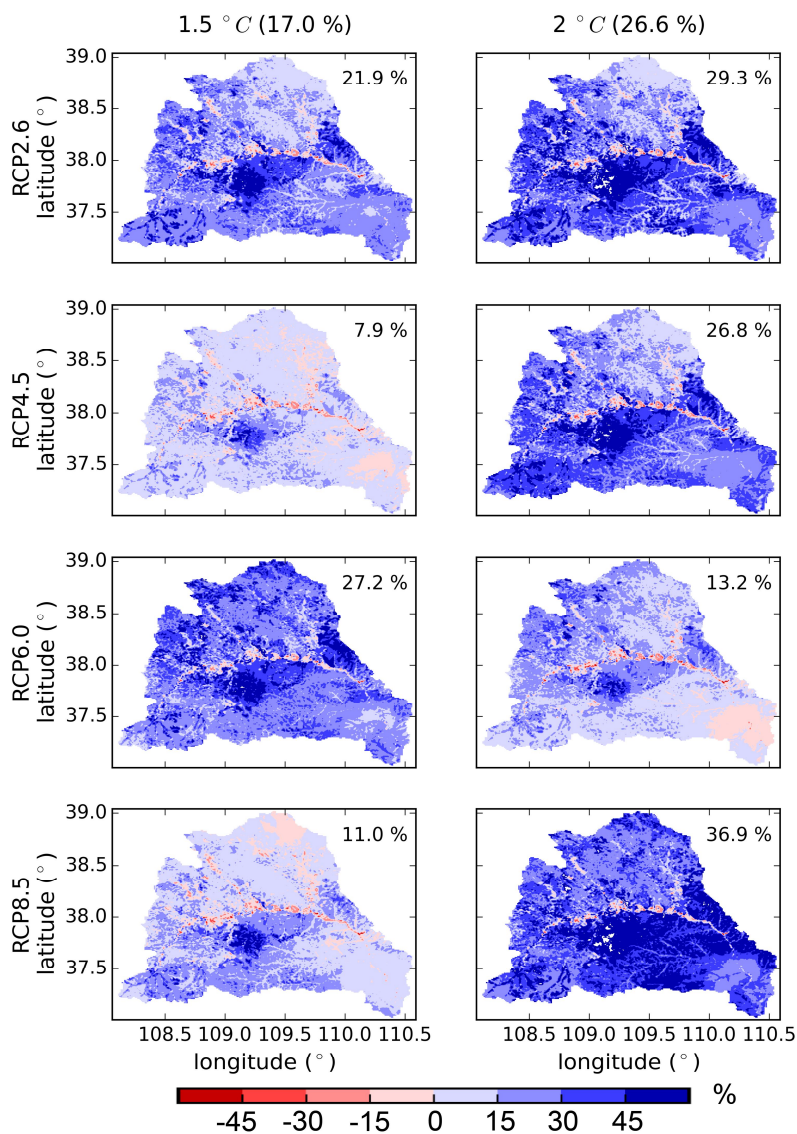
617

618 **Figure 3.** Historical (ALL) and future (RCP2.6/4.5/6.0/8.5) time series of
619 standardized annual mean (a) temperature, (b) precipitation and (c) streamflow, and (d)
620 the time series of hydrological drought frequency (drought months for each year) over
621 the Wudinghe watershed. Shaded areas indicate the ranges between maximum and
622 minimum values among CMIP5/CLM-GBHM model simulations. ALL represents
623 historical simulations with both anthropogenic and natural forcings,
624 RCP2.6/4.5/6.0/8.5 represent four representative concentration pathways from lower
625 to higher emission scenarios.



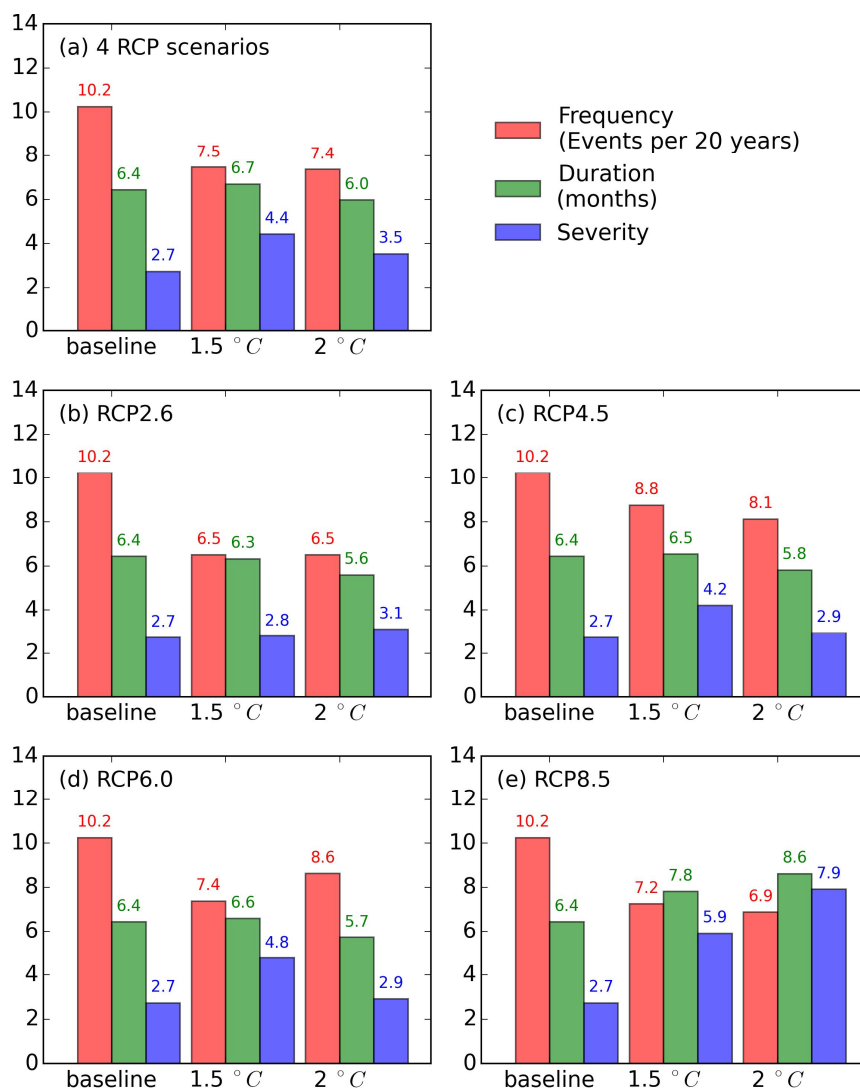
626

627 **Figure 4.** Spatial pattern of relative changes in multi-model ensemble mean
 628 precipitation at 1.5 °C and 2 °C warming levels compared to the baseline period
 629 (1986-2005). The percentages in the upper-right corners of each panel are the
 630 watershed-mean changes for different RCP scenarios, and the percentages in the top
 631 brackets are the mean values from four RCP scenarios.



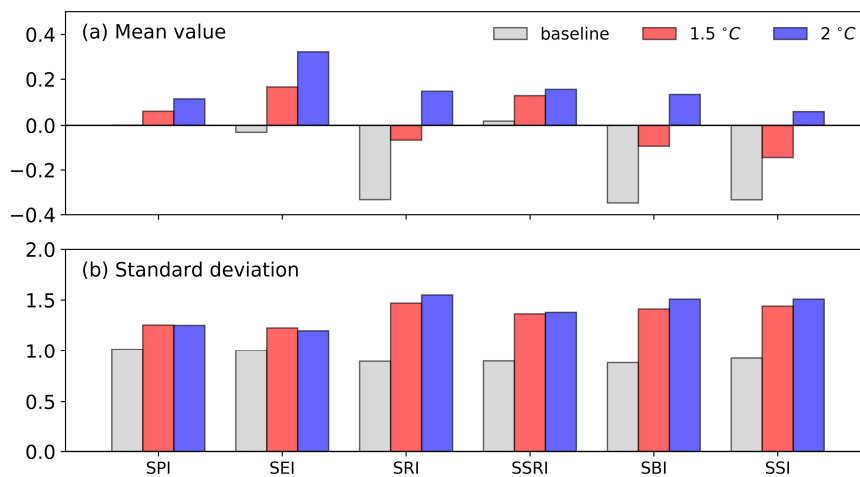
632

633 **Figure 5.** The same as **Figure 4**, but for the spatial patterns of runoff changes.



634

635 **Figure 6.** Comparison of the characteristics (frequency (number of drought events per
 636 20 years), duration (months) and severity) averaged among climate models and RCP
 637 scenarios for hydrological drought events during the baseline period (1986-2005) and
 638 the periods reaching 1.5 °C and 2 °C warming levels.



639

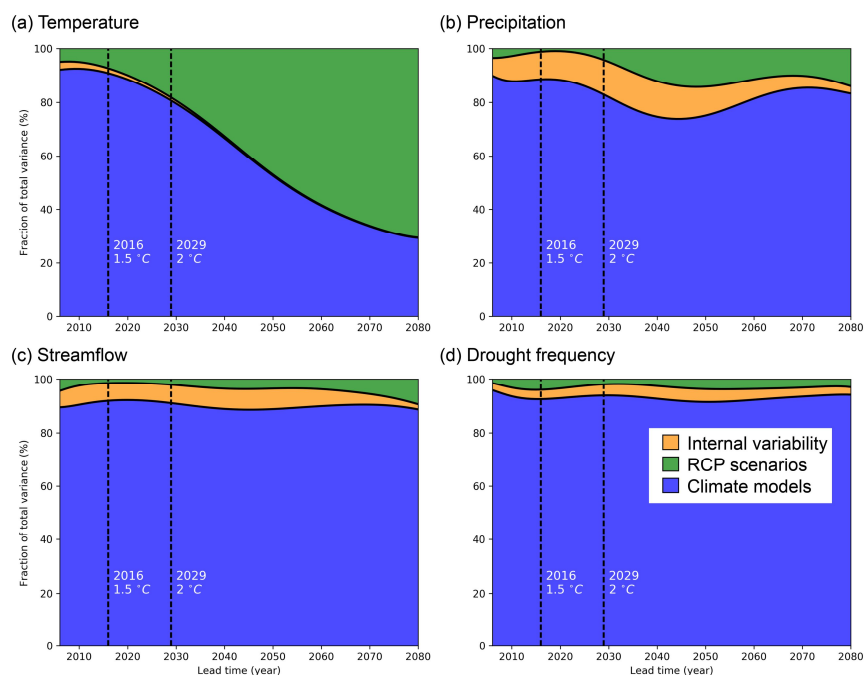
640 **Figure 7.** Comparison of (a) mean values and (b) standard deviations for hydrological

641 indices averaged among climate models and RCP scenarios during the baseline period

642 (1986-2005) and the periods reaching 1.5 °C and 2 °C warming levels. SPI, SEI, SRI,

643 SSRI, SBI, SSI represent standardized indices of precipitation, evapotranspiration,

644 runoff, surface runoff, baseflow (subsurface runoff) and streamflow, respectively.



645

646 **Figure 8.** Fractions of uncertainties from internal variability (orange), RCP scenarios
647 (green) and climate models (blue) for the projections of 20-years moving averaged (a)
648 temperature, (b) precipitation (c) streamflow and (d) hydrological drought frequency.
649 Two dashed lines indicate the multi-model ensemble median years reaching 1.5 °C
650 (year 2016) and 2 °C (year 2029) warming levels, respectively.



651 **Table 1.** CMIP5 model simulations used in this study. ALL represents historical simulations with both anthropogenic and natural forcings
 652 (r1i1p1 realization), RCP2.6/4.5/6.0/8.5 represent four representative concentration pathways from lower to higher emission scenarios.

GCMs	Institute	Resolution	Historical simulations	RCP scenarios
GFDL-CM3	NOAA GFDL	144×90	ALL	RCP2.6/4.5/6.0/8.5
GFDL-ESM2M	NOAA GFDL	144×90	ALL	RCP2.6/4.5/6.0/8.5
HadGEM2-ES	MOHC	192×145	ALL	RCP2.6/4.5/6.0/8.5
IPSL-CM5A-LR	IPSL	96×96	ALL	RCP2.6/4.5/6.0/8.5
IPSL-CM5A-MR	IPSL	144×143	ALL	RCP2.6/4.5/6.0/8.5
MIROC-ESM-CHEM	MIROC	128×64	ALL	RCP2.6/4.5/6.0/8.5
MIROC-ESM	MIROC	128×64	ALL	RCP2.6/4.5/6.0/8.5
MRI-CGCM3	MRI	320×160	ALL	RCP2.6/4.5/6.0/8.5



653 **Table 2.** Trends in hydrometeorological variables and hydrological drought frequency over the Wudinghe watershed. Historical observed trends
 654 for streamflow and drought frequency were calculated by using naturalized streamflow data (Yuan et al., 2017). Here, “**” and “***” indicate 90%
 655 and 99% confidence levels, respectively, while those without any “*” show no significant changes ($p > 0.1$).

Historical (1961-2005) and future (2006-2099) scenarios	Changing trend of standardized timeseries (yr^{-1})			
	Temperature	Precipitation	Streamflow	Drought frequency
(historical) observations	0.0494**	-0.0216*	-0.0503**	0.0448**
(historical) all forcings simulations	0.0272**	-0.0009	-0.0213**	0.0346**
(future) RCP2.6 simulations	0.0138**	0.0025*	0.0046**	-0.0069**
(future) RCP4.5 simulations	0.0291**	0.0056**	0.0105**	-0.0096**
(future) RCP6.0 simulations	0.0312**	0.0039**	0.0038**	-0.0044**
(future) RCP8.5 simulations	0.0345**	0.0108**	0.0133**	-0.0107**



656 **Table 3.** Determination of crossing year for the periods reaching 1.5°C and 2 °C warming levels for different GCMs and RCPs combinations.
 657 Here, “NR” means that the corresponding GCM/RCP combination will not reach the specified warming level throughout the 21st century.

GCMs	1.5 °C warming level				2 °C warming level			
	RCP2.6	RCP4.5	RCP6.0	RCP8.5	RCP2.6	RCP4.5	RCP6.0	RCP8.5
GFDL-CM3	2016	2016	2016	2016	2021	2016	2018	2016
GFDL-ESM2M	2031	2023	2030	2023	NR	2048	2064	2041
HadGEM2-ES	2016	2016	2016	2016	2020	2036	2023	2024
IPSL-CM5A-LR	2016	2018	2016	2016	2033	2028	2038	2026
IPSL-CM5A-MR	2016	2016	2016	2016	2037	2025	2033	2023
MIROC-ESM-CHEM	2016	2021	2016	2016	2022	2031	2032	2026
MIROC-ESM	2017	2017	2017	2017	2025	2029	2025	2023
MRI-CGCM3	2047	2028	2045	2024	NR	2049	2060	2040
Model ensemble	2016	2018	2016	2016	2029	2030	2033	2025
Total ensemble	2016				2029			



658 **Table 4.** Uncertainty contributions (%) from internal variability, climate models and RCPs scenarios for the future projections considering 1.5 °C
 659 and 2 °C warming levels.

Variables	1.5 °C warming level			2 °C warming level		
	Internal variability	Climate Models	RCPs scenarios	Internal variability	Climate Models	RCPs scenarios
Temperature	2.0	90.1	8.0	1.2	80.5	18.4
Precipitation	10.0	88.1	2.0	12.5	82.8	4.8
Streamflow	6.7	91.2	2.1	6.9	90.9	2.3
Drought frequency	3.4	93.3	3.3	4.1	93.4	2.5